JOURNAL OF APPLIED POLYMER SCIENCE VOL. 12, PP. 191-212 (1968)

Calendering Thermoplastic Materials

J. S. CHONG,
Research and Development Division,
E. I. du Pont de Nemours & Co., Inc., Parlin, New Jersey

Synopsis

A general equation for the true shear rate encountered in calendering non-Newtonian fluids is derived. Based on several constitutive equations (for a power-law, a three-constant Oldroyd, and a modified second-order Rivlin-Ericksen fluid), calendering is analyzed from the hydrodynamic point of view. The significance of dimensionless groups (the Deborah number, the Weisenberg numbers, and the viscoelastic ratio number), consisting of rheological and kinematic parameters, is discussed for scaling from prototype to production calendering. Correlation of experimental data obtained by using laboratory and production calenders is presented, and the scaling criteria obtained from the theory are examined. The onset of unstable flow, which causes non-uniform internal strain patterns (nerve) in calendered sheeting, is discussed in terms of the Weisenberg number. Good and poor calendering regions for a polymer are discussed qualitatively by using a dynamic response diagram, and the importance of the overall calendering conditions on the final sheeting quality is discussed.

INTRODUCTION

A theoretical analysis of fluid flow between a pair of rotating rolls was made by Ardichvili[1] in 1938 on the basis of the Reynolds lubrication theory of Newtonian hydrodynamics. Later Eley,[2] Gaskel,[3] Atkinson and Nancarrow,[4] Paslay,[5] Kneschke,[6] McKelvey[7] and, more recently, Tokita and White[8] analyzed the problem of calendering or milling independently. Gaskel's approach is basically similar to that of Ardichvili, but his solutions for velocity and pressure distributions between two rolls and for the roll-separating force are more elaborate, and he extends the solution to the calendering of Bingham plastics. Atkinson and Nancarrow and McKelvey treat the problem of calendering power-law fluids. Paslay's analysis is essentially based on Oldroyd's fluid model[9,10] with three rheological constants. Although the results of Paslay's analysis indicate how certain parameters of elastic properties are interrelated with the kinematic parameters in calendering, he neglects the normal stress effects in the equation of motion.

Tokita and White reviewed some of these papers in their studies on milling several elastomers. They observed a striking dependence of the rheological behavior of elastomers on milling temperature. They classify the rheological behaviors of elastomers in milling into four different

temperature regions. The first two regions discussed by them seem to be relatively insignificant in calendering, but the last two regions are of interest in calendering. The region in which an elastomer seems like an opaque bag is called region 3, and the region in which an elastomer on a mill flows like a viscous fluid with little elastic recovery is called region 4. In terms of Tobolsky's[11] method of characterizing the viscoelastic behavior of amorphous polymers these regions correspond to the rubbery plateau and viscous flow regions. The authors point out the significance of two dimensionless groups, the Deborah number and the Weisenberg number, which characterize the viscoelastic behavior of the materials in milling or calendering. Although they have indicated that the equations of motion in milling or calendering viscoelastic materials can be analyzed by using a second-order Rivlin-Ericksen asymptotic expansion, the resulting equations even without inertia terms are nonlinear, and they have not been able to obtain solutions for velocity and pressure distributions or for the roll-separating force.

In our study thermoplastic materials are treated as purely viscous non-Newtonian fluids or as non-Newtonian viscoelastic materials. In the first case the dependence of apparent viscosity on shear rate is fully considered; in the second, which is a modification of the purely viscous non-Newtonian fluid, the effect of elastic properties is considered. Also included in this study is a dynamic similarity, or scaling, analysis for the flow of viscoelastic fluids in geometrically similar calenders. Furthermore, experimental data obtained by using a laboratory and a production calender are correlated, based on the theory developed, and the scaling criteria developed in the theory are examined.

THEORETICAL DEVELOPMENT

Calendering is a continuous sheet-forming operation utilizing more than a pair of driven rolls, and a mass of softened thermoplastic materials is formed into a sheet of uniform thickness.[12] When thermoplastic materials are calendered, the primary effect occurring in the polymer is laminar shear deformation.[7] Usually four equal-size rolls are employed in calendering. These rolls are arranged either in inverted L type or inclined Z type, and their speed, nip opening, and temperature can be controlled independently. The temperatures of the first two rolls are usually kept either at the transition region or the rubbery-plateau region, whereas the temperatures of the last rolls are kept near the viscous-flow region.

Figure 1 shows a schematic diagram of the last two rolls from which the final sheeting comes out. The theoretical development for calendering and the pertinent experimental data that will be discussed later all refer to these rolls.

A rheological equation for the simplest type of non-Newtonian behavior, in which the complications caused by time of shear and strain are absent, may be described by the following equation:

$$du/dy = F(\tau) \tag{1}$$

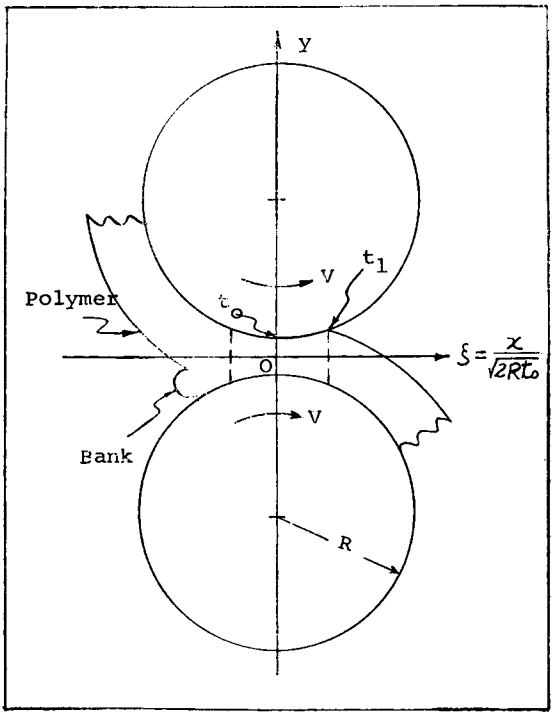

Fig. 1. Schematic diagram of calender rolls and coordinates.

Integrating the above equation for the case of equal roll speeds

$$V - u = \int_t^{t_w} du = t_0(1 + \xi^2) \int_\tau^{\tau_w} F(\tau)(d\tau/\tau_w) \tag{2}$$

where V is the calender roll speed, τ_w is the wall shear stress, and ξ is a dimensionless distance in calendering direction. The volumetric flow rate per unit width of sheeting can be obtained by integrating eq. (2).

$$Q = 2\int_0^{t_w} u\, dy$$

$$= 2t_0(1 + \xi^2)[V - t_0(1 + \xi^2)/\tau_w^2 \int_0^{\tau_w} \tau(F)\, \tau d\tau] \tag{3}$$

It is interesting to notice in eq. (3) that the flow rate consists of two terms; the first term on the right side of the equation is due to the drag flow and is independent of the rheological properties, whereas the second term is due to the pressure flow. The second term can be positive or negative, depending on the direction of fluid velocity component. If the equation of continuity is used, the volume flow rate must be equal to

$$Q = 2Vt_1 = 2Vt_0(1 + \xi^2) \tag{4}$$

where t_1 is one-half of the sheeting thickness. Substituting this equation into eq. (3) and rearranging, we obtain

$$3V(\xi_1^2 - \xi^2)/t_0(1 + \xi^2)^2 = (3/\tau_w^2) \int_0^{\tau_w} \tau F(\tau)\, d\tau \tag{5}$$

The term on the left side of the equation has a dimension equivalent to shear rate and is equal to the wall sheai rate for a Newtonian fluid. This equation suggests immediately that there are two regions in the nip where the shearing rates are zero. These regions occur on both sides of the nip where $\xi = \pm\xi_1$. By differentiating eq. (5) with respect to the wall shear stress τ_w and rearranging we can show that the true shear rate at the wall is given by the following equation:

$$F(\tau_w) = (3V/t_0)[(\xi_1^2 - \xi^2)/(1 + \xi^2)^2]\{2/3 + d \ln [3V(\xi^2 - \xi_1^2)/ t_0(1 + \xi^2)^2]/(3\, d \ln \tau_w)\} \tag{6}$$

For a Newtonian fluid the logarithmic term should be equal to unity, and eq. (6) reduces to

$$\dot{\gamma}_w = (3V/t_0)[(\xi_1^2 - \xi^2)/(1 + \xi^2)^2] \tag{7}$$

The true shear rate at the wall for non-Newtonian fluids is given by eq. (6), which may be written

$$F(\tau_w) = (3V/t_0)[(\xi_1^2 - \xi^2)/(1 + \xi^2)^2]\ [(2n + 1)/3n] \tag{8}$$

where n is the reciprocal of the logarithmic term in eq. (6). Equation (8) describes the wall shear rate encountered in calendering in terms of the kinematics of calendering and the flow behavior index. The flow behavior index n can be obtained from capillary rheometer data by measuring the slope of the flow curves plotted on a log–log scale. Examination of eq. (8) shows that the maximum shear rate occurs at the nip where $\xi = 0$:

$$(\dot{\gamma})_{\max} = (3V/t_0)\xi_1^2[(2n + 1)/3n] \tag{9}$$

In the determination of the rheological behavior of a thermoplastic material with a capillary rheometer, eq. (9) gives an upper limit of the shear rate of interest in calendering.

For an expression for the roll-separating force an equation for the pressure distribution has to be obtained. If we neglect inertia and normal stress terms in the equation of motion,[13,14] the pressure is

$$P = \sqrt{(2R/t_0)} \int_{\xi_1}^{\xi} \tau_w\langle\xi\rangle/(1 + \xi^2)(d\xi) \tag{10}$$

where $\tau_w\langle\xi\rangle$, the shear stress at roll surface, is a function of the dimensionless distance ξ. If a rheological equation for a polymer is specified, then the integration above can be performed. The roll-separating force per unit width of sheeting can be obtained by integrating eq. (10) with respect to ξ,

$$F/W = \sqrt{(2R/t_0)} \int_{\xi_1}^{\xi^*} \int_{\xi_1}^{\xi} [\tau_w\langle\tau_w\rangle/(1 + \xi^2)]\, d\xi\, d\xi \tag{11}$$

where ξ^* satisfies a condition $P(\xi^*) = 0$. A solution of this equation for Newtonian fluids was obtained by Gaskel and appears in several books,[7,12,15] but for a non-Newtonian fluids a rheological equation that correctly represents the relationship between shear stress and shear rate encountered in calendering must be selected. Several rheological equations that may be used for representing the flow behavior of most thermoplastic materials are the following.

A power-law equation:[7,13]

$$\sigma = -PI + K[{}^1/_2 \text{ tr } B_1^2]^{(n-1)/2} B_1 \tag{12}$$

A three-constant Oldroyd equation:[9,10]

$$\sigma = -PI + \tau \tag{13}$$

where $\tau + \lambda_1 (\mathfrak{D}\tau/\mathfrak{D}t) = 2\mu_0[e + \lambda_2 (\mathfrak{D}e/\mathfrak{D}t)]$ and $\mathfrak{D}/\mathfrak{D}t$ is the Jaumann derivative.

A modified second-order Rivlin-Ericksen equation:[8,16]

$$\sigma = -PI + K[{}^1/_2 \text{ tr } B_1^2]^{(n-1)/2} B_1 + \omega_2 B_1^2 + \omega_3 B_2 \tag{14}$$

where I is the unit matrix, and B_1 and B_2 are acceleration tensors. For laminar shear flow they are

$$B_1 = \begin{vmatrix} 0 & \dot{\gamma} & 0 \\ \dot{\gamma} & 0 & 0 \\ 0 & 0 & 0 \end{vmatrix}, \qquad B_2 = (-2) \begin{vmatrix} \dot{\gamma}^2 & 0 & 0 \\ 0 & 0 & 0 \\ 0 & 0 & 0 \end{vmatrix}$$

CALENDERING POWER-LAW FLUID

Although calendering power-law fluids has been treated by several authors,[4,7] a theoretical limitation of the fluid model, its consequence in the correlating of experimental data, and a predicted stagnation envelope in the forward region of the nip have not been discussed heretofore. Furthermore, correlation of experimental data for the roll-separating force as a function of calendering variables predicted by this fluid model does not appear in the literature. We shall discuss these matters in an orderly way, develop an equation for the roll-separating force, and later discuss its validity in the correlation of experimental data.

Inspection of eq. (8) shows that the shearing rates at calender roll surface are zero at $\xi = \pm\xi_1$ and become maximum at the nip. We find experimentally that the power-law does not represent the flow behavior of polymer melts in range of shear rates of interest. Although the power-law model is not satisfactory for the complete analysis of velocity field in calendering, it is simple and adequately describes most of the viscous flow behavior of many thermoplastic materials over a wide range of shear rates. We shall first apply this fluid model to the hydrodynamic analysis of calendering and later consider several other fluid models for viscoelastic materials.

For fluids obeying eq. (12) the momentum equation,[13,14] neglecting the inertia terms, reduces to

$$\partial P/\partial x = Kn|\partial u/\partial y|^{n-1}(\partial^2 u/\partial y^2) \tag{15}$$

An expression for the local velocity profile in the polymer between two rolls can be obtained by integrating this question:

$$u = [K/(\partial p/\partial x)][n/(1+n)][(1/K)(\partial p/\partial x)y + C_1]^{1+(1/n)} + C_2 \tag{16}$$

If we assume that two rolls are equal in size and moving at the same velocity without slip, the constants C_1 and C_2 can be evaluated readily, and the velocity distribution is

$$u = V + [n/(1+n)][(1/K)(\partial P/\partial x)]^{1/n}[y^{1+(1/n)} - t^{1+(1/n)}] \tag{17}$$

The volume flow rate per unit width of sheeting is obtained by integrating eq. (17) with respect to y:

$$Q = 2\int_0^t u\,dy = 2t[V - [n/(1+2n)](1/K)(\partial P/\partial x)^{1/n}t^{1+(1/n)}] \tag{18}$$

$$= 2Vt_1$$

A dimensionless form for the velocity profile can be obtained from eqs. (17) and (18) by eliminating the pressure-gradient term:

$$u/V = 1 + [(1+2n)/(1+n)][(\xi_1^2 - \xi^2)/(1+\xi^2)^{2+(1/n)}] \times [(1+\xi^2)^{1+(1/n)} - (y/t_0)^{1+(1/n)}] \tag{19}$$

If $n = 1.0$ this equation reduces to the velocity profile for Newtonian fluids. The equation shows that the maximum velocity at the nip is

$$(u/V)_{\max} = 1 + [(2n+1)/(1+n)]\xi_1^2 \tag{20}$$

A schematic diagram of the velocity profiles is shown in Figure 2. Examination of eq. (19) reveals some interesting flow patterns around the nip area. In the region where $-\xi_1 < \xi < +\xi_1$ the velocity profile is convex, because the pressure gradient is negative. In the region where $\xi < -\xi_1$ the pressure gradient becomes positive, and the forward fluid motion is retarded, causing the velocity profile to be concave. As ξ decreases, a point is eventually reached where the fluid velocity at the mid-plane becomes zero. This stagnation point is found by setting eq. (19) equal to zero at $y = 0$:

$$\xi_s = -\{\xi_1^2 - [(1+n)/(2+3n)]\}^{1/2} \tag{21}$$

In the region where $\xi < -\xi_s$ eq. (19) shows that the velocity component changes sign as y varies for a given value of ξ. This suggests that, near the mid-plane fluid moves away from the nip of the rolls because the velocity components are negative but that near the roll surface the velocity components are positive and the fluid moves toward the nip. The net result is a partial circulation of fluid in the region $\xi < -\xi_s$. This circulation

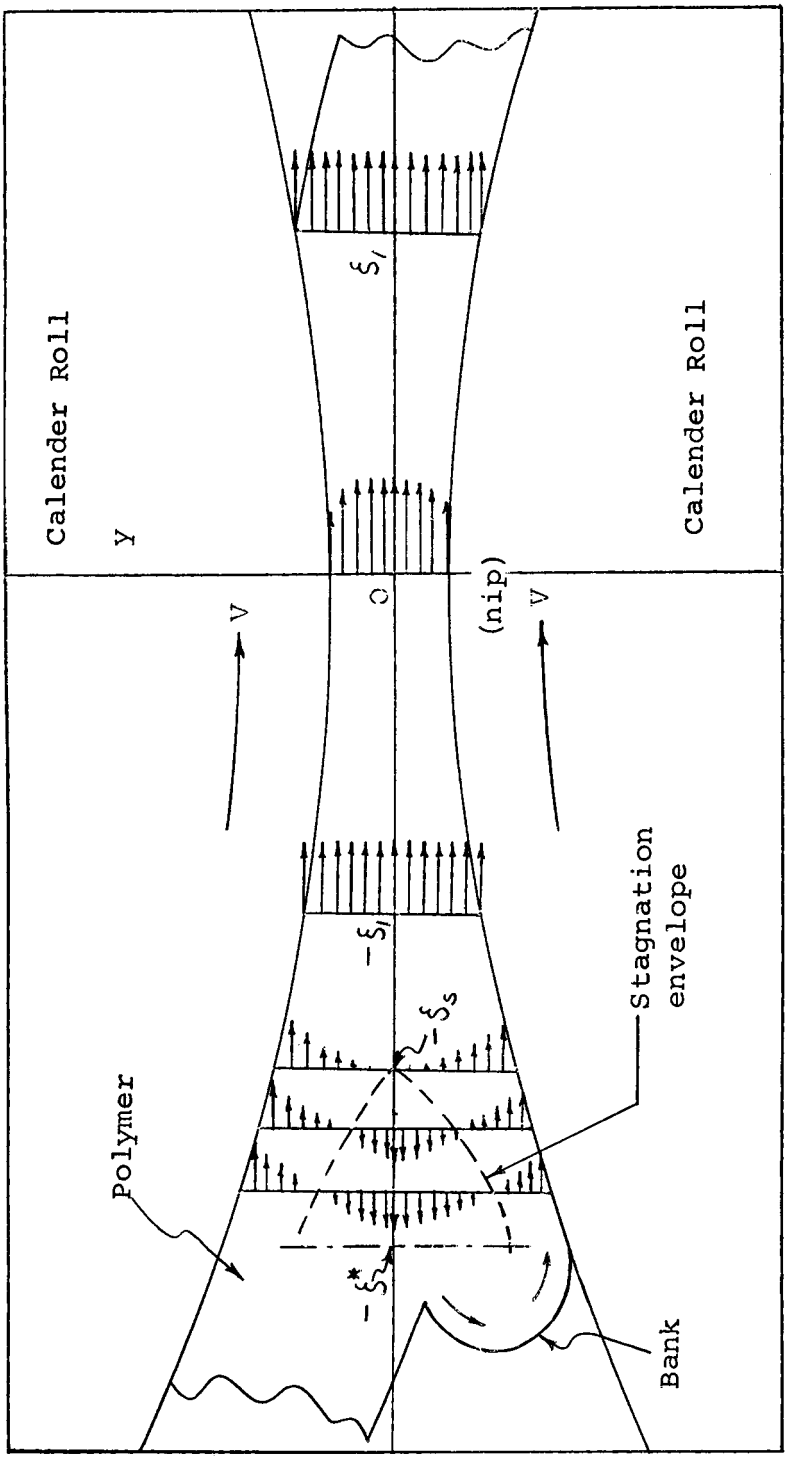

Fig. 2. Schematic diagram of velocity distributions and stagnation envelope.

should form closed cellular vortices in the rotating bank. The stream function[13] for the vortices can be obtained by integrating the velocity distribution function given by eq. (19):

$$\psi = [2V\eta t_0/\delta(1+n)]\{n_2^{1+(1/n)}(\xi^2 - \xi_1^2)/(1+\xi^2)^{2+(1/n)} + [(1+n) + (1-2n)\xi_1^2 - n\xi^2]/(1+\xi^2)\} \quad (22)$$

If $n = 1$, this equation reduces to the stream function obtained by Bergan for milling Newtonian fluids.[12] Actually, there are an infinite number of stagnation points that form an envelope. We shall call this the "stagnation envelope." The locus of the stagnation envelope may be obtained from eq. (19) by setting it equal to zero and solving for y:

$$(y/t_0)_s = (1+\xi^2)\{1 + [(1+n)/(1+2n)] \times [(1+\xi^2)/(\xi_1^2+\xi^2)]\}^{n/(1+n)} \quad (23)$$

A schematic diagram of the stagnation envelope is also shown in Figure 2.

The pressure distribution can be obtained readily from eq. (18). The equation can be rearranged into the following form:

$$\partial P/\partial\xi = (2KV^n/\delta t_0^n)[(1+2n)/n][|\xi^2 - \xi_1^2|^{n-1}(\xi^2 - \xi_1^2)/(1+\xi^2)^{2n+1}] \quad (24)$$

Equation (24) shows that the pressure gradients at $\xi = \pm\xi_1$ are zero. Since ξ_1 is defined as the point where the polymer sheeting loses contact with the roll surface, the pressure at that point is equal to zero or to a datum pressure. Therefore, the maximum pressure occurs shortly before the nip, where $\xi = -\xi_1$. The same result is obtained for Newtonian fluids.

Integrating eq. (24) with respect to ξ gives pressures as a function of distance in the direction of calendering:

$$P = (2KV^n/\delta t_0^n)[(1+2n)/n]^n \times \int_{\xi_1}^{\xi} [|\xi^2 - \xi_1^2|^{n-1}(\xi^2 - \xi_1^2)/(1+\xi^2)^{2n+1}]d\xi \quad (25)$$

This equation shows that the pressure is proportional to the nth power of roll speed and inversely proportional to the $(n + {}^1/_2)$th power of the nip opening. Comparison of eq. (25) with the equivalent expression for Newtonian fluids shows that in calendering non-Newtonian fluids the pressure is relatively insensitive to small changes in calendar speed and nip opening. Equation (25) cannot be integrated to give an analytical form, but a graphical method may be used readily.

The maximum pressure at $\xi = -\xi_1$ can be calculated from eq. (25) by rearranging to give

$$P = (-2KV^n/\delta t_0^n)[(1+2n/n)]^n\xi_1^{2n+1}\int_0^1 |1-\rho^2|^n d\rho/(1+\xi_1^2\rho^2)^{2n+1} \quad (26)$$

where $\xi = \xi_1\rho$. At $\xi = -\xi_1$ the equation reduces to

$$P_{max} = (4KV^n/\delta t_0^n)[(1 + 2n)/n]^n \xi_1^{2n+1} \int_0^1 |1 - \rho^2|^n d\rho/(1 + \xi_1^2\rho^2)^{2n+1} \tag{27}$$

The pressure at the nip, where $\xi = 0$, is

$$P_{nip} = (2KV^n/\delta t_0^n)[(1 - 2n)/n]^n \xi_1^{2n+1} \times \int_0^1 |1 - \rho^2|^n d\rho/(1 + \xi_1^2\rho^2)^{2n+1} \tag{28}$$

Equations (27) and (28) show that the pressure at the nip is one-half of the maximum pressure at $\xi = -\xi_1$, and this relationship is independent of the rheological properties.[7]

The roll-separating force per unit width of sheeting can be obtained by integrating equation (25):

$$F/2RW = K(V/t_0)^n[(1 + 2n)/n]^n \times \int_{\xi_1}^{\xi^*} \int_{\xi_1}^{\xi} |\xi^2 - \xi_1^2|^{n-1}(\xi^2 - \xi_1^2)d\xi/d\xi(1 + \xi^2)^{2n+1} \tag{29}$$

Because of the fractional power appearing in the integrand an analytical expression for the roll-separating force cannot be obtained in a closed form. However, for a given value of the flow behavior index n eq. (29) can be

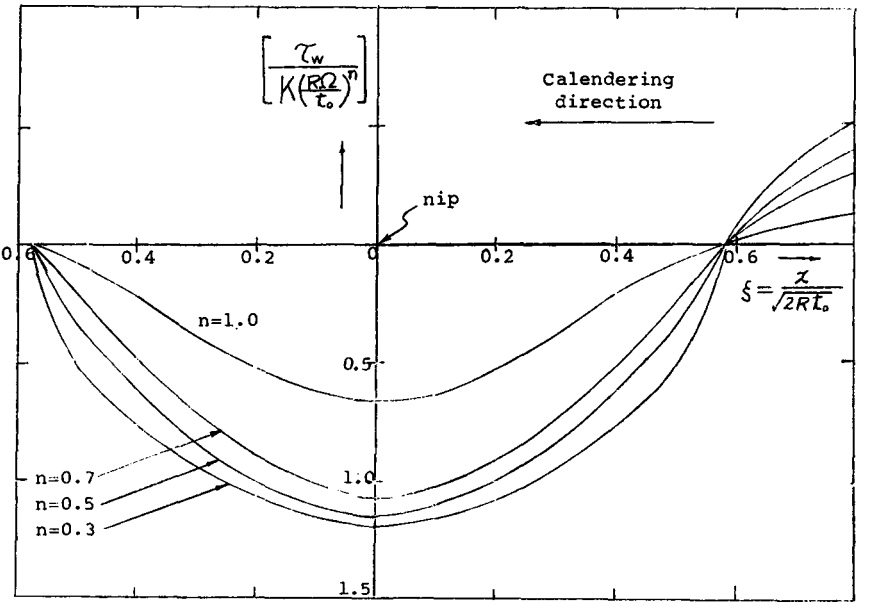

Fig. 3. Dimensionless wall shear stress as a function of dimensionless distance for various flow behavior indices.

evaluated easily by graphical integration. Therefore, if the composition of a polymer to be calendered is kept constant, the last term in the equation will be approximately constant for a given calender. This indicates, then, that if the roll-separating force per unit width of calendered sheeting is plotted against V/t_0 on a log–log scale, a straight line should be obtained at each calendering temperature.

It should be pointed out here that the validity of the power-law equation for calendering cannot be judged by comparing experimentally observed roll-separating forces with those calculated from eq. (29). Experimentally determined pressure distributions should be compared with the values calculated by using eq. (25). Agreement between calculated roll-separating forces and experimental values does not necessarily mean that the actual pressure distribution is the same as predicted by a theoretical equation. This point has been overlooked in the past by several investigators.[12,17]

The shear stress at the roll surface can be obtained readily by substituting eq. (24) into

$$\tau_w = \int_0^{t_w} (\partial P/\partial x)dy$$

$$= K(V/t_0)^n[(1 + 2n)/n]^n[|\xi^2 - \xi_1^2|^{n-1}(\xi^2 - \xi_1^2)/(1 + \xi^2)^{2n+1}] \quad (30)$$

Figure 3 shows the dependence of the wall shear stress on dimensionless distance for several values of the flow behavior index.

CALENDERING VISCOELASTIC FLUIDS

An Oldroyd Fluid

Oldroyd[9] proposed an eight-constant model to describe non-Newtonian viscosity, normal stresses, and oscillatory phenomena of incompressible fluids. Williams and Bird[10] showed that a special three-constant version of this model also describes these features. The stress components for the three-constant Oldroyd equation are

$$\sigma_{xx} = -P + \mu_0(\lambda_1 - \lambda_2)\dot{\gamma}^2/(1 + \lambda_1^2\dot{\gamma}^2) \quad (31)$$

$$\sigma_{yy} = -P - \mu_0(\lambda_1 - \lambda_2)\dot{\gamma}^2/(1 + \lambda_2^2\dot{\gamma}^2) \quad (32)$$

$$\tau_{xy} = \mu_0(1 + \lambda_1\lambda_2\dot{\gamma}^2)\dot{\gamma}/(1 + \lambda_2^2\dot{\gamma}^2) \quad (33)$$

where μ_0 is a lower limiting viscosity, and λ_1 and λ_2 are relaxation and retardation times, respectively. Substitution of these stress components into the stress equations of motion without inertia terms, we obtain

$$(1/\mu_0)(\partial P/\partial x) = (\partial/\partial x)[(\lambda_1 - \lambda_2)\dot{\gamma}^2/(1 + \lambda_1^2\dot{\gamma}^2)] + (\partial/\partial y)[(1 + \lambda_1\lambda_2\dot{\gamma}^2)\dot{\gamma}/(1 + \lambda_1^2\dot{\gamma}^2)] \quad (34)$$

$$(1/\mu_0)(\partial P/\partial y) \approx (\partial/\partial y)[(\lambda_1 - \lambda_2)\dot{\gamma}^2/(1 + \lambda_1^2\dot{\gamma}^2)] \quad (35)$$

Numerical solutions of eq. (34) without the normal stress term have been computed by Paslay for several values of the relaxation time λ_1 ranging from 10^{-3} to 3.15×10^{-4} sec.

From eqs. (34) and (35) we find that the shear rate must satisfy the following relationship:

$$(\partial^2/\partial y^2)[(1 + \lambda_1\lambda_2\dot{\gamma}^2)\dot{\gamma}/(1 + \lambda_1^2\dot{\gamma}^2)] \approx 2(\partial^2/\partial x\partial y)[(\lambda_1 - \lambda_2)\dot{\gamma}^2/(1 + \lambda_1^2\dot{\gamma}^2)] \quad (36)$$

Equations (34) and (35) are nonlinear, and analytical expressions for velocity and pressure distributions cannot be obtained. However, an approximate method of calculating pressure distribution and the resulting roll-separating force is to use the velocity distribution for Newtonian fluids.

We obtain some useful information for scale-up based on these equations. If we transform the equations in terms of dimensionless parameters by introducing

$$V^* = u/V \qquad \eta = y/(2Rt_0)^{1/2}$$
$$V^{**} = v/V \qquad \lambda_1^* = \lambda_1/\theta$$
$$\xi = x/(2Rt_0)^{1/2} \qquad \lambda_2^* = \lambda_2/\theta$$

where θ is the duration of deformation in calendering and λ_1^* and λ_2^* are the ratios of characteristic times to processing time. The significance of this ratio, the Deborah number, in processing viscoelastic materials has been pointed out by Pawelski[18] and more recently by White and others.[8,16,19,20]

If we introduce these dimensionless variables into eqs. (34) and (35), we obtain

$$\partial P/\partial\xi = \mu_0(R\Omega/2t_0)\theta\Omega(\lambda_1^* - \lambda_2^*) \times \{(\partial V^*\partial\eta)^2/[1 + \lambda_1^{*2}\theta^2\Omega(R\Omega/2t_0)(\partial V^*/\partial\eta)^2]\} + \Omega\mu_0(R/2t_0)^{1/2}[1 + \theta^2\lambda_1^*\lambda_2^*(R\Omega/2t_0)(\partial V^*/\partial\eta)^2](\partial V^*/\partial\eta)/[1 + \lambda_1^{*2}\theta^2\Omega(R\Omega/2t_0)(\partial V^*/\partial\eta)^2] \quad (37)$$

$$\partial P/\partial\eta = -\mu_0(R\Omega/2t_0)\theta\Omega(\lambda_1^{*2} - \lambda_1^{*2}) \times \{(\partial V^*/\partial\eta)^2/[1 + \lambda_1^{*2}\theta^2\Omega(R\Omega/2t_0)(\partial V^*/\partial\eta)^2]\} \quad (38)$$

where Ω is the angular velocity.

In the scaling of a prototype model based on laboratory calender data, if we wish to maintain the polymer residence time θ constants, the angular roll speed must be kept the same. Under these conditions eqs. (37) and (38) show that the pressure distribution will be similar if the ratio of roll diameter to nip opening is the same.

The ratio of normal stress difference to shear stress can be obtained readily from eqs. (31), (32), and (33):

$$(\sigma_{xx} - \sigma_{yy})/\tau_{xy} = (2)^{1/2}\theta\Omega(R/t_0)^{1/2} \times \{(\lambda_1^* - \lambda_2^*)(\partial V^*/\partial\eta)/[1 + \lambda_1^*\lambda_2^*\theta^2\Omega(R\Omega/2t_0)(\partial V^*/\partial\eta)^2]\} \quad (39)$$

This ratio is called the Weisenberg number by White and others.[16,19,21] We notice here that maintaining a constant ratio of roll diameter to nip opening to obtain the same pressure gradient is equivalent to maintaining the same Weisenberg number. The Weisenberg number appears to be an important parameter for the onset of non-uniform internal strain patterns (nerve) in calendered sheeting. This will be discussed in the Experimental section.

A MODIFIED SECOND-ORDER RIVLIN-ERICKSEN FLUID

An obvious modification of the power-law model is to use a more sophisticated constitutive equation, such as the asymptotic expansion of Rivlin-Ericksen fluid, as later modified by White and his co-workers[21] to take into account the shear rate dependence of non-Newtonian viscosity. The modified second-order model results from assuming that the kinematics of all past times within the fluid's memory can be described by a truncated Taylor series about the present time. This permits removing the kinematic parameters from the hereditary integrals and the expression of stress in terms of instantaneous deformation rates and acceleration. The equation, which predicts most of the important nonlinear flow aspects, including non-Newtonian viscosity and normal stresses, has the form

$$\sigma = -PI + K[{}^1/_2 \operatorname{tr} B_1^2]^{(n-1)/2} B_1 + \omega_2 B_1^2 + \omega_3 B_2 \tag{40}$$

where K and n denote the usual power-law parameters and ω_2 and ω_3 are additional physical-property parameters that determine the magnitude of the normal stress functions in steady laminar shear flow.

It is really questionable whether such assumptions can be justified in calendering polymer melts. The relaxation time of polymer melts at a calendering temperature is usually much greater than the duration of deformation in calendering. For example, if we were to calender 10 mil sheeting with 24-in. diameter rolls at 10 ft./min., the average polymer residence time between the rolls would be about 2 sec.; this is much smaller than the relaxation time of most polymer melts at a processing temperature.[22]

If eq. (40) is substituted into the equation of motion without inertia terms for the modified second-order viscoelastic materials, then we have

$$\nabla P = K\nabla\cdot[{}^1/_2 \operatorname{tr} B_1^2]^{(n-1)/2} B_1 + \omega_2\nabla\cdot B_1^2 + \omega_3\nabla\cdot B_2 \tag{41}$$

On the basis of the order-of-magnitude analysis[8] the stress components can be obtained from eq. (40). They are:

$$\tau_{xy} = K(\partial u/\partial y)^n + \omega_3[u(\partial^2 y/\partial x\partial y) + v(\partial^2 u/\partial y^2) + 2(\partial u/\partial x)(\partial u/\partial y)] + \ldots \tag{42}$$

$$\sigma_{xx} = (\omega_2 - 2\omega_3)(\partial u/\partial y)^2 + \ldots \tag{43}$$

$$\sigma_{yy} = \omega_2(\partial u/\partial y)^2 + \ldots \tag{44}$$

Substituting eqs. (42), (43), and (44) into eq. (41), we obtain the equations of motion in the x and y directions. They are

$$\partial P/\partial x = Kn(\partial u/\partial y)^{n-1}(\partial^2 u/\partial y^2) + \omega_3(\partial/\partial y)[u(\partial^2 u/\partial x \partial y) + v(\partial^2 u/\partial y^2) + 2(\partial u/\partial x)(\partial u/\partial y)] \quad (45)$$

$$\partial P/\partial y = 2(\omega_2 - 2\omega_3)(\partial u/\partial y)(\partial^2 u/\partial y^2) \quad (46)$$

It should be noticed that eq. (45) reduces to the case of calendering power-law fluids, if the rheological constants for viscoelastic properties are zero.

If we introduce the dimensionless variables defined previously in eq. (45), we obtain

$$\begin{aligned}(1/K)1/[\Omega^n(R/t_0)]^{n/2}(\partial P/\partial \xi) = {} & [n/(2)^{1/2}](\partial V^*/\partial \eta)^{n-1}(\partial^2 V^*/\partial \eta^2) \\ & - [N_{we}/2(R/t_0)^{1-n/2}](\partial/\partial \eta)[V^*(\partial^2 V^*/\partial \xi \partial \eta) \\ & + V^{**}(\partial^2 V^*/\partial \eta^2) + 2(\partial V^*/\partial \xi)(\partial V^*/\partial \eta)] \\ & + [N_{we}/(R/t_0)^{1-n/2}](2 - N_{vr})(\partial V^*/\partial \eta)(\partial^2 V^*/\partial \xi \partial \eta) \quad (47)\end{aligned}$$

where $N_{we} = (-1)(\omega_3/K)(R/\Omega t_0),^{2-n}$ the Weisenberg number, and $N_{vr} = \omega_2/\omega_3$, the viscoelastic ratio number.

In eq. (47) we find several significant dimensionless parameters; they are the Weisenberg number, the viscoelastic ratio number, the flow behavior index, and the ratio of roll diameter to nip opening. The physical significance of the Weisenberg number was discussed earlier. The viscoelastic ratio number denotes the ratio of forces due to the square of the first acceleration tensor to the second acceleration tensor.[16]

If the angular roll speed and the ratio of roll diameter to nip opening were kept constant between prototype and production calender, this would be equivalent to maintaining both the same Weisenberg number and the Deborah number.

Comparison of eqs. (37) and (47) shows that only the viscoelastic ratio number does not appear in the former equation. Very little experimental data exist for ω_2, and the significance of this number in processing polymer melts is not known. According to White,[23] this ratio appears to be very small and may be neglected in eq. (47).

In the foregoing analyses we have used different fluid models to obtain scale-up criteria for calendering. We notice here that, if the constitutive equations are relatively simple and yet depict the general viscoelastic properties, the resulting criteria are essentially the same.

EXPERIMENTAL RESULTS AND DISCUSSION

Polymer and Rheological Properties

The polymer used in calendering is a high molecular weight cellulose acetate derivative with several plasticizers.

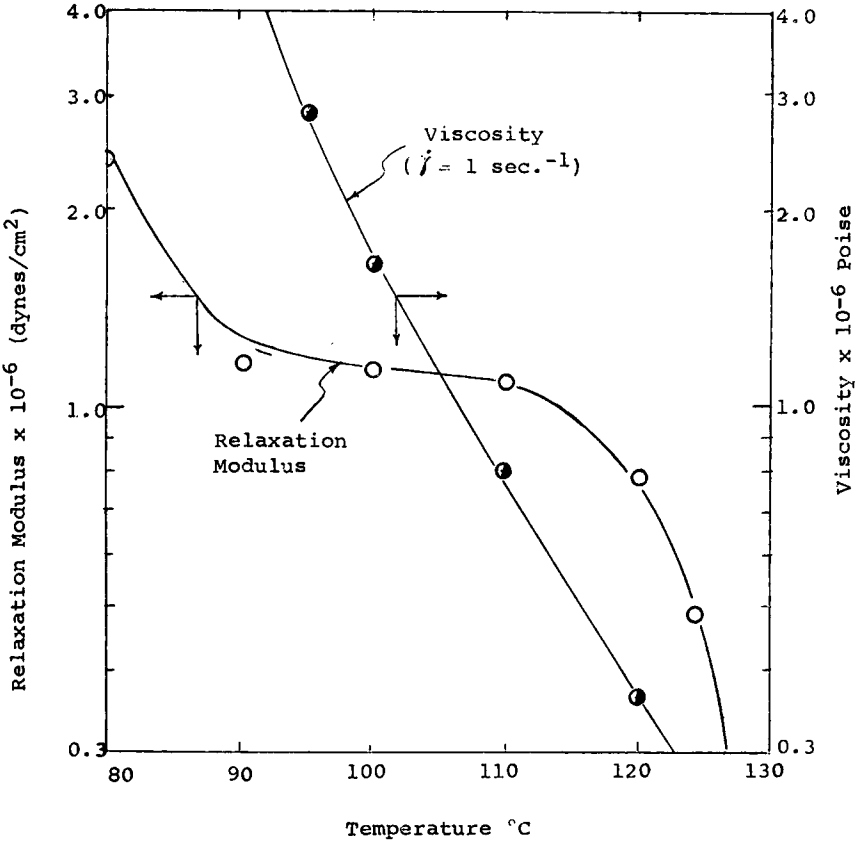

Fig. 4. Relaxation modulus and low-shear viscosity of a polymer as a function of temperature.

Capillary rheometer data for the polymer show that the flow behavior of the polymer at calendering temperatures follows the power-law equation for several orders of magnitude of shear rate. At low shear rates, however, the polymer appears to behave like a Bingham plastic rather than a Newtonian one.

Relaxation moduli and low shear viscosities of the polymer as a function of temperature are shown in Figure 4. The figure shows that the calendering temperatures, which ranged from 90 to 140°C., fall in the rubbery plateau and viscous-flow regions. The figure gives us some idea of the order of magnitude of the polymer relaxation time at these temperatures.

Polymer Calendering

The polymer was calendered at various temperatures and speeds. The roll-separating force, nip opening, and dimensions of calendered sheeting were measured at each speed. The resulting data are shown in Figure 5. The calender used in obtaining the data shown in this figure has four

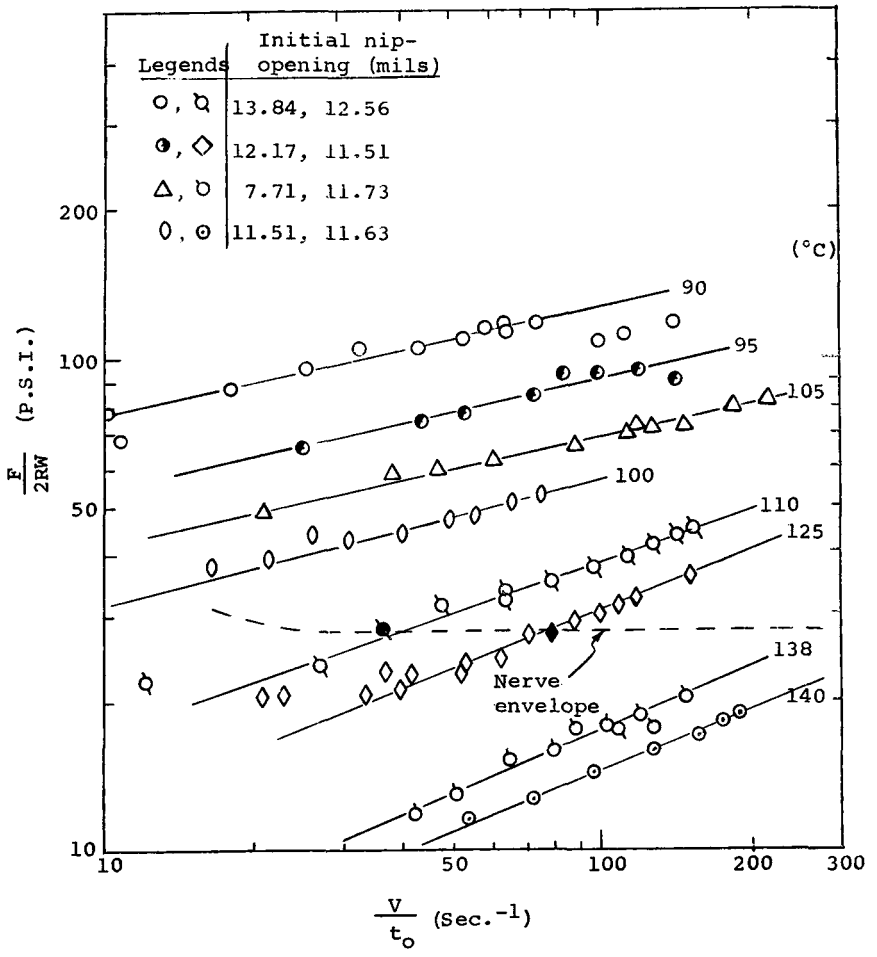

Fig. 5. Laboratory calender data. The black points represent calender speeds at which "nerve" appeared in sheeting.

equal rolls (8 × 16 in.) with an inverted L-shaped roll arrangement. In all experiments the temperature of the feed rolls was kept at 90°C., while the temperatures of the last two rolls were varied. The initial nip opening at each temperature was measured by inserting several pieces of solder at different points across the last two rolls.

If we assume that the double-integration term in eq. (29) is fairly constant and independent of roll speeds, a straight-line relationship between $F/2RW$ and V/t_0 on a log–log scale should be expected. The slope of these lines should be equal to the flow behavior index n, obtained from capillary rheometer data. We found that the flow behavior index determined from calendering data was slightly lower than that based on capillary rheometer data. This discrepancy is caused by a slight increase in nip opening due to large roll-separating forces at increased speeds. The data

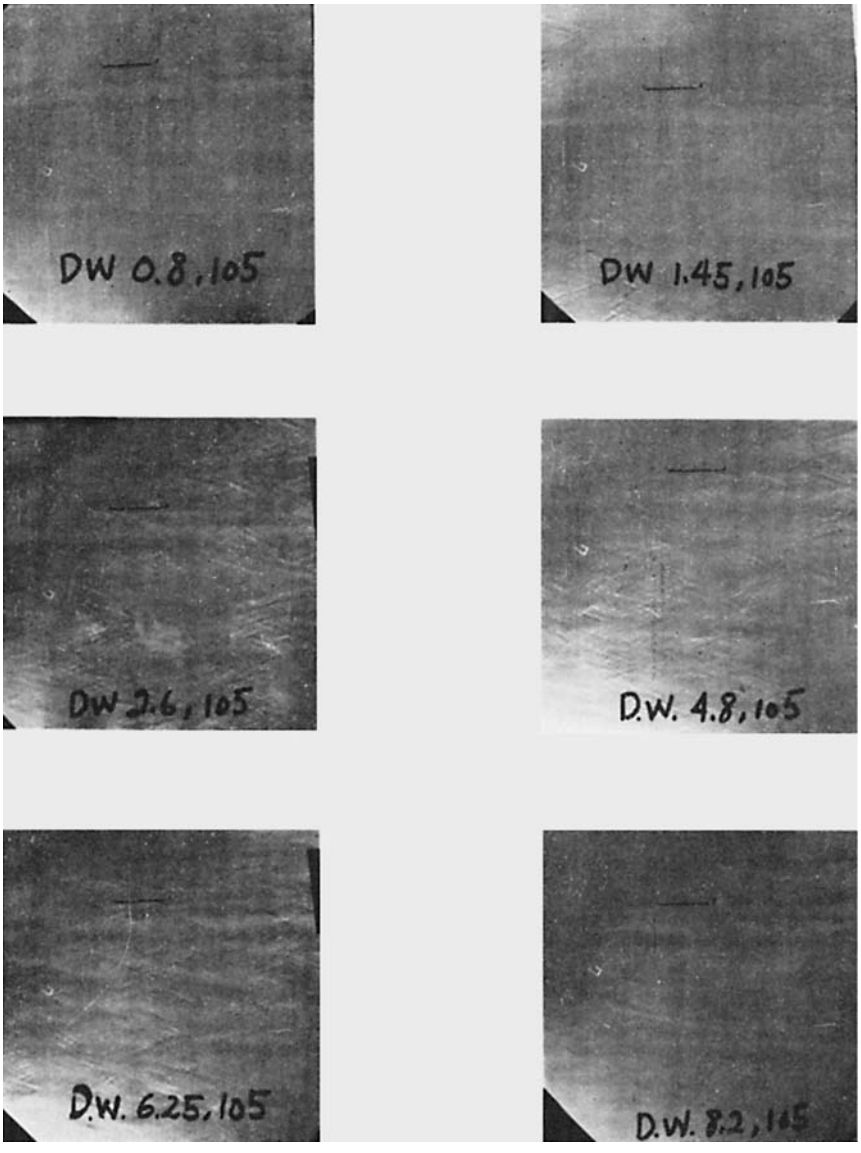

Fig. 6. Internal strain patterns (nerve) in calendered sheeting. The first number in each picture denotes calender speed in feet per minute, and the second denotes temperature in degrees centigrade. The scale in each picture represents 1 in.

in the figure show that the roll-separating force decreases remarkably as the temperature is increased. In terms of eq. (29), this is because the temperature dependence of the consistency index K follows the Arrhenius type of formula.

Onset of Nerve and Unstable Flow

At a given temperature there is a certain speed at or above which the calendered sheeting showed the so-called nerve when examined with polarized light. The nerve is due to the non-uniform strain patterns in sheeting. As the roll temperature is increased while the nip opening is maintained constant, nerve appears at higher speeds. Figure 5 shows the calendering speeds at which nerve appeared in sheeting at 110 and 125°C. Above these temperatures sheeting calendered at a maximum speed (about 11 ft./min.) does not show any nerve patterns. Figure 6 shows several photographs of nerve patterns obtained under different calendering conditions.

Above 110°C. these internal strains were found to occur at a constant value of $F/2RW$, independent of calendering temperature. However, below 110°C. the value decreased as the temperature increased. The temperature dependence of the critical roll-separating force $(F/2RW)_c$ at which nerve appears in sheeting seems to be closely related to that of the critical wall shear stress at which melt fracture is observed in a capillary rheometer. The critical shear stresses at which the extrudate surface appears distorted were measured by using capillary tubes with different

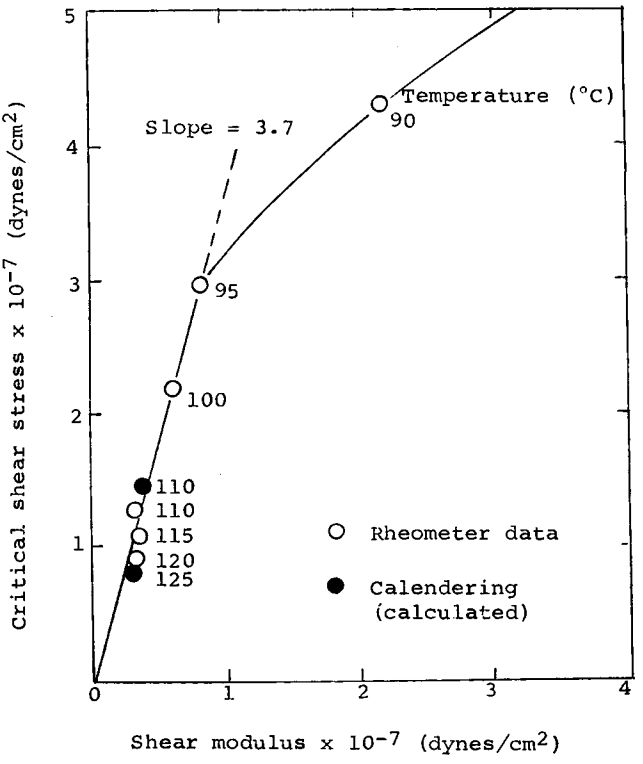

Fig. 7. Critical shear stress as a function of shear modulus at the onset of melt fracture in capillary extrusion and in calendering.

entrance angles. Although the mode of surface distortion appeared to be highly dependent on the entrance angle, the stresses at which the extrudate appears distorted were independent of the entrance angle. However, the critical stress below 115°C. was highly temperature-dependent. The Bagley-Tordella melt-fracture criteria[23–25] do not seem to apply to our polymer at temperatures below 115°C.

On the conjecture that nerve is due to non-uniform strain patterns and that the kinematic mechanism for the onset of these strain patterns is similar to the melt-fracture phenomena, we have plotted critical shear

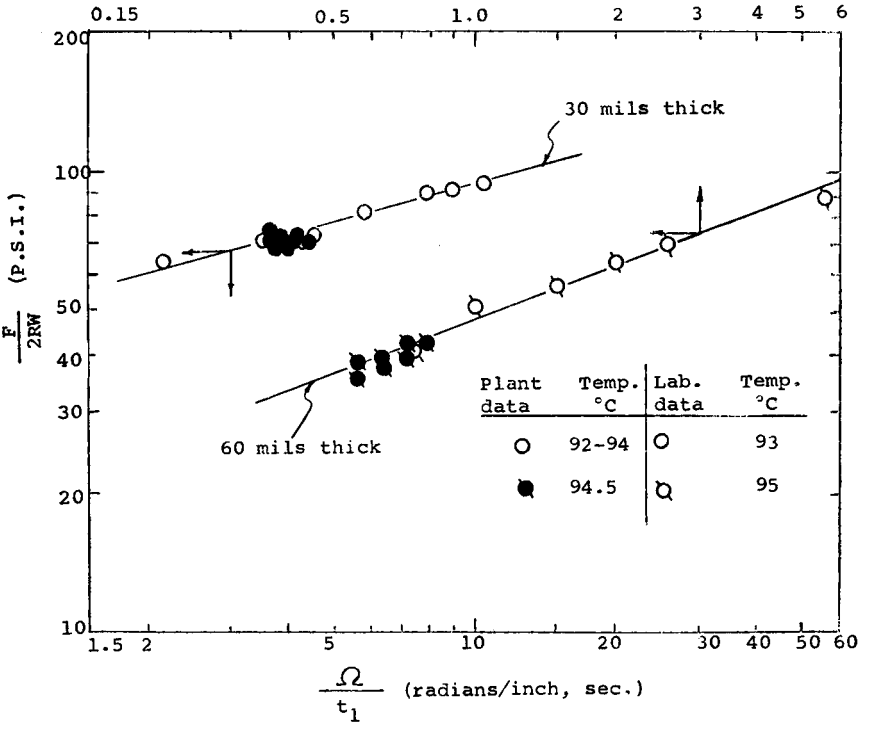

Fig. 8. Correlation of prototype and production calender data.

stresses observed with a capillary rheometer as a function of calculated elastic shear modulus[26,27] at pertinent shear rates. These data are shown in Figure 7. In the figure the critical wall shear stresses at the nip calculated with the use of eq. (30) are also plotted as a function of shear modulus at several calendering conditions. The slope of the line is equal to the recoverable elastic strain at which nerve appears in the sheeting. According to White,[28] the recoverable strain is equivalent to the Weisenberg number. The calculated elastic strain at the onset of nerve is about 3.7 and seems to be approximately in the same order of magnitude found by other investigators[23–25] for the extrusion of several different polymers through a capillary tube.

Correlation Between Prototype and Production Calender Data

The roll-separating force of a small laboratory calender can be correlated with a large-sized production calender in terms of angular roll speed. Figure 8 shows such correlations for several different thicknesses of sheeting. It should be noticed in the figure that sheeting thickness is used instead of nip opening.

In the light of the scaling criteria for calendering viscoelastic materials discussed earlier these data show that, as far as roll-separating force as a function of roll speed is concerned, it does not seem to be necessary to maintain the ratio of roll diameter to nip opening of prototype and production calenders. It seems to be sufficient to maintain the same angular speed between laboratory and production calenders. This is equivalent to maintaining a constant Deborah number.

The onset of nerve in production calendering was not investigated in this study. However, we believe that the R/t_0 ratio has a significant effect on the onset of nerve and the extent and severeness in calendered sheeting. This will be further investigated in the future.

Polymer Calenderability

The commonly used word "calenderability" is very difficult to define in terms of the rheological properties of a given polymer and the kinematics of polymer deformation encountered in calendering. There is no doubt

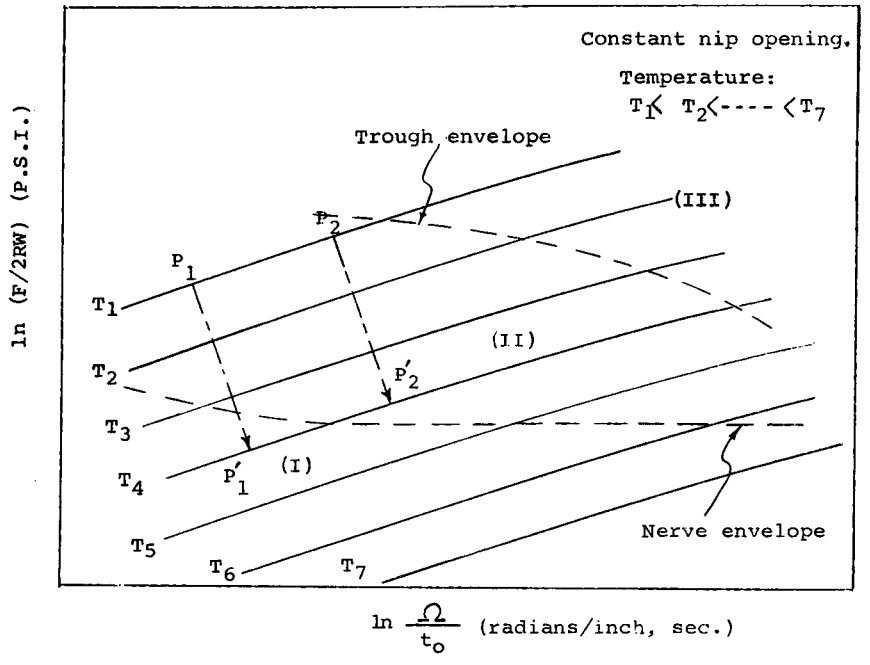

Fig. 9. Schematic diagram of calenderable regions of a polymer.

that the chemical composition of polymer plays an important part in imparting a good sheeting surface.

In the past the judgment of calenderability at a given temperature was based largely on the physical quality of the final calendered sheeting and on the appearance of the bank and its rotational motion. The physical quality was judged according to the amount of troughs and the severeness and extent of nerve in the sheeting. These defects were found to be highly dependent on roll-separating force, calender speed, temperature, and appearance of the bank and its rotational motion. Tearing banks, the segment rotating in inconsistent directions, are highly undesirable. In general, a relatively small bank, rotating as shown in Figure 2, with a smooth surface is indicative of good calenderability.

Large roll-separating forces and slow calender speeds were found to be essential in eliminating air bubbles. However, we found that the onset of nerve was most sensitive to calendering temperature. It appears that nerve is similar to the melt-fracture phenomena commonly observed in extruding polymer melts.

From our study we can now define a good calenderability region of a given polymer in a more precise manner. Figure 9 shows a schematic diagram of several different calenderability regions. In the figure a family of straight lines at each temperature can be constructed on the basis of eq. (29). These lines are divided by two envelopes; the upper one may be called a trough envelope and the lower one a nerve envelope. It is possible to locate the trough envelope in the diagram based on the hydrodynamic treatment of air-bubble deformation in highly viscous fluid. However, the nerve envelope cannot be located theoretically until we know more about the kinematics of deformation of viscoelastic materials.

Let us consider points P_1 and P'_1 shown in the diagram. The calendering condition at P_1 may correspond to feed rolls that are kept at relatively low temperature. The polymer at P_1 will eventually pass the final rolls at P'_1. The temperature at this point is higher than P_1, while the nip opening is less than the feed rolls. Since P_1 falls in the region 1 below the nerve envelope, the final sheeting should be free of nerves and troughs. Consider, however, P_2 and P'_2 at different calendering speeds. The calendering conditions of the last rolls is such that P'_2 falls in region 2, where nerve appears in sheeting but no troughs appear. Region 3 would be the most undesirable for calendering, since sheeting produced in this region would show severe nerve patterns and troughs. This shows how the operating conditions of rolls before the final rolls are made affects the quality of final products.

I am grateful to my colleagues of the Parlin Research and Development Division, E. I. Du Pont de Nemours & Co., Inc., for their interest in the publication of this work. I am indebted to M. F. Valania for his suggestions and assistance in the experimental portion of this work.

Nomenclature

e	Strain tensor
P	Hydrostatic pressure
R	Roll radius
t_0	One half of nip opening
t_w	$= t_0 (1 + \xi^2)$, curvature of roll surface
W	Sheeting width
δ	$= y/(2Rt_0)^{1/2}$ dimensionless
ξ	$= x/(2Rt_1)^{1/2}$ dimensionless.
σ	Stress tensor

Only those notations which are not defined in the text are listed here.

References

1. G. Ardichvili, *Kautschuk*, **14**, 23 (1938).
2. D. D. Eley, *J. Polymer Sci.*, **1**, 535 (1946).
3. R. E. Gaskel, *J. Appl. Mech.*, **17**, 334 (1950).
4. E. B. Atkinson and H. A. Nancarrow, *Plastics Inst. (London), Trans. J.*, **19**, 23 (1951).
5. P. R. Paslay, *J. Appl. Mech.*, **24**, 602 (1957).
6. von A. Kneschke, *Freiberger Forschungsh. B*, **16**, 5 (1957).
7. J. M. McKelvey, *Polymer Processing*, Wiley, New York, 1962.
8. N. Tokita and J. L. White, *J. Appl. Polymer Sci.*, **10**, 1011 (1966).
9. J. G. Oldroyd, *Proc. Roy. Soc. (London) Ser. A*, **200**, 523 (1950).
10. M. C. Williams and R. B. Bird, *Phys. Fluids*, **5**, No. 9, 1126 (1962).
11. A. V. Tobolsky, *Properties and Structure of Polymers*, Wiley, New York, 1960.
12. E. C. Bernhardt, Ed., *Processing of Thermoplastic Materials*, Reinhold, New York, 1959.
13. R. B. Bird, W. E. Stewart, and E. N. Lightfoot, *Transport Phenomena*, Wiley, New York, 1960.
14. H. Schlichting, *Boundary Layer Theory*, 4th Ed., McGraw-Hill, New York, 1960.
15. W. L. Wilkinson, *Non-Newtonian Fluids*, Pergamon, London, 1960.
16. J. L. White and A. B. Metzner, *A.I.Ch.E. J.*, **11**, 324 (1965).
17. R. H. Carley, *S.P.E. (Soc. Plastics Engrs.) Trans.*, **2**, 265, (1962).
18. von O. Pawelski, *Rheol. Acta*, **2**, 273 (1962).
19. J. L. White and N. Tokita, *J. Appl. Polymer Sci.*, **11**, 321 (1967).
20. A. B. Metzner, J. L. White, and M. M. Denn, *A.I.Ch.E. J.*, **12**, No. 5, 868 (1966).
21. A. B. Metzner, J. L. White, and M. M. Denn, *Chem. Eng. Progr.*, **62**, No. 12, 81 (1966).
22. C. J. Aloisio and S. Matsuoka, *J. Polymer Sci. A-2*, **4**, 113 (1966).
23. J. P. Tordella, *J. Appl. Polymer Sci.*, **7**, 215 (1963).
24. E. B. Bagley and H. P. Schreiber, *Trans. Soc. Rheol.*, **5**, 341 (1961).
25. R. S. Spencer, *J. Polymer Sci.*, **5**, 591 (1950).
26. S. Onogi, H. Kato, and S. Ueki, in *U. S.–Japan Seminar in Polymer Physics (J. Polymer Sci. C*, **15**), R. S. Stein and S. Onogi, Eds., Interscience, New York, 1966, p. 481.
27. W. P. Cox and E. H. Merz, *J. Polymer Sci.*, **28**, 619 (1958).
28. J. L. White, *J. Appl. Polymers Sci.*, **8**, 2339 (1964).

Résumé

Une équation générale pour la vitesse de cisaillement vrai rencontrée au cours du calandrage de fluides non-Newtoniens a été déduite. Sur la base de plusieurs équations

de constitution, le calandrage est analysé du point de vue hydrodynamique. La signification des groupes sans dimensions (le nombre de Deborah, les nombres de Weisenberg, et le nombre du rapport viscoélastique) contenant des paramètres rhéologiques et cinématiques est discutée pour passer du prototype au calandrage de production. La corrélation des résultats expérimentaux obtenus en utilisant des calandres de laboratoire et de production est présentée et des critères obtenus au départ de la théorie sont examinés. Le début de l'écoulement instable qui cause des réseaux de tension internes non-uniformes au course de la formation de feuilles par calandrage est discuté sur la base du nombre de Weisenberg. Les régions de calendrage bonnes et pauvres pour un polymère sont discutées qualitativement en utilisant le diagramme de réponse dynamique et l'importance des conditions générales de calandrage sur la qualité des feuilles finalement obtenues est discutée.

Zusammenfassung

Für die wahre Schergeschwindigkeit, die beim Kalandern nicht-Newtonscher Flüssigkeiten auftritt, wurde eine allgemeine Gleichung abgeleitet. Das Kalandern wird, vom hydrodynamischen Gesichtspunkt aus, auf der Basis verschiedener grundlegender Gleichungen (für eine Potenzgesetz-, eine drei-Konstanten-Oldroyed- und eine modifizierte Rivlin-Ericksen-Flüssigkeit zweiter Ordnung) analysiert. Die Bedeutung der aus rheologischen und kinematischen Parametern bestehenden dimensionslosen Gruppen (der Deborah-Zahl, der Weisenberg-Zahlen und der viskoelastischen Verhältniszahl) beim Übergang vom prototypischen zum produktionsmässigen Kalandern wird diskutiert. Es wird eine Korrelation der mittels Labor- und Produktionskalandern ermittelten Daten gebracht, und die aus der Theorie erhaltenen Kriterien für die Übertragbarkeit werden geprüft. Das Einsetzen eines instabilen Flusses, der ungleichförmige innere Spannungsmuster (Adern) in kalanderten Platten hervorruft, wird an Hand der Weisenberg-Zahl diskutiert. Gute und schlechte Kalanderbereiche für ein Polymeres werden qualitativ an Hand eines dynamischen Reaktionsdiagrammes erörtert, und die Wichtigkeit der Gesamtbedingungen des Kalanderns für die Endqualität der Platten wird diskutiert.

Received June 26, 1967
Prod. No. 1684